Memoirs of the Faculty of Engineering, Okayama University, Vol.36, No.2, pp.73-82, March 2002

Application of Transfer Matrix Method with Signal Flow-Chart to Analyze Optical Multi-Path Ring-Resonator

Iip Syarif HIDAYAT[1),*], Yoshitaka TOYOTA[2)], Osamu TORIGOE[3)],
Osami WADA[1)] and Ryuji KOGA[1)]

[1)] Graduate School of Natural Science and Technology, Okayama University
[2)] Departement of Communication Network Engineering, Okayama University
[3)] Departement of Electrical and Electronic Engineering, Okayama University
3-1-1 Tsushima-naka, Okayama 700-8530, Japan

A multi-path ring-resonator (MPRR) was proposed to extend FSR of ring resonator. However, it is complicated to analyze the MPRR by using well-known analysis techniques such as scattering matrix or other numerical methods. This paper describes procedure for deriving transfer matrix by means of signal flow-chart to analyze the MPRR. We do not need complicated calculation for steady state analysis because transfer matrix elements are formulated clearly. As a result, The calcultaion time in this method can be reduced 1/3 to 1/20 times compared with using scattering matirx method. Furthermore, a transmittance characteristics of the MPRR at FSR extension-factor of 10 will also be shown. This suggests that analysis of other types of the MPRR by using this method can be performed simply and take a shorter time.

1 INTRODUCTION

Ring resonators have proven to be one of the most versatile elements for various applications, as evidenced by their wide spread use in electronic and microwave circuits. Recently, on the field of integrated optics, study on waveguide-type optical ring-resonator has also grown rapidly because of compact and frequency tuning can be easily achieved by using a suitable guided-wave control technique. Some authors have successfully fabricated micrometer order ring-resonators [1], [2]. These results suggest that ring resonators should be expected as a potential device for optical signal processing, such as DWDM communication system. This system requires a wide free spectral range (FSR). Since FSR of ring resonator is inversely propotional to ring radius, a wider FSR can be realized by reducing ring radius. However, it is well known that the bending loss of a waveguide increases rapidly with decreasing the radius of curvature. Therefore, extending FSR in ring resonator increases insertion loss. We proposed the MPRR as a candidate method to extend FSR without decreasing ring radius [3]. We reported in [4] that the MPRR has advantages of size, compared to conventional double-cavity ring-resonator [5], and crosstalk and extension factor of FSR, compared to triple-coupler ring-resonator [6].

There are various methods to evaluate the characteristics of the MPRR such as FDTD method [7], or scattering matrix method [5]. The first has advantage of time- and space-variant result but needs a large computer memory and much time to calculate. The second needs complicated matrix operation, especially for the multi-path structure of ring resonator. This disadvantage can be avoided by means of transfer matrix method. Transfer matrix method has been used widely for the analysis of, for example, cascaded fiber-optic recirculating and nonrecirculating delay lines

*E-mail iip@dev.cne.okayama-u.ac.jp

[8]. The aim of this paper is to provide a derivation of transfer function of MPRR using signal flow-chart.

2 PRINCIPLE OF THE MPRR

The structure of the MPRR is schematically depicted in Fig.1. The MPRR consists of an inner ring with radius r, an outer ring, two waveguides for input and output, and four directional couplers. The input waveguide is coupled to the inner ring by means of directional coupler with power coupling ratio of K_1. The inner and outer ring coupled each other by means of two directional couplers with power coupling ratios of K_3 and K_4. The MPRR has two output ports. One is an output port of directional coupler with power coupling ratio K_1 (Out-1), and the other one is an output waveguide coupled to the inner ring by directional coupler with power coupling ratio K_2 (Out-2). The resonance light will pass through the Out-2 port and the antiresonance light will pass through the Out-1 port. We suppose that directional couplers have zero length. It means that phase shift effect in directional couplers is neglected in this study. We also assume that there is no frequency independence at power coupling ratio of directional couplers.

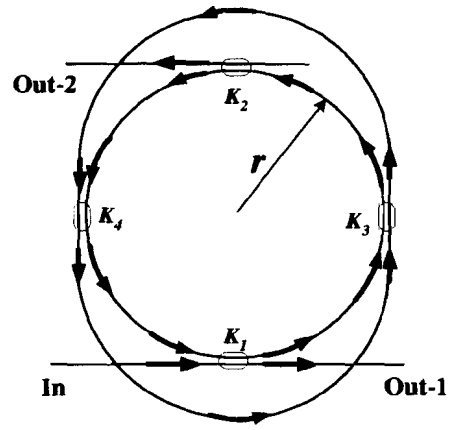

Figure 1: Basic structure of MPRR.

Although the light in MPRR propagate in various routes (this is the reason why we call Fig.1 as a multi-path ring-resonator), there are only three basic closed loops in the MPRR if we set upper part and lower part of the outer ring symmetrical to the directional couplers with power coupling ratios K_3 and K_4. The first one is a closed loop of the inner ring with loop length of Λ_1. The second is a closed loop which consists of a half of the inner ring and a half of the outer ring with loop length of Λ_2. The last is a closed loop of the outer ring with loop length of Λ_3. The FSR of each loop, which is defined as the frequency spacing between two neighboring resonant frequencies, can be written as follows:

$$\Delta\nu_i = \frac{c}{n_e \Lambda_i} \qquad i = 1, 2, 3 \tag{1}$$

where c is the free-space velocity of light, n_e is effective refractive index of waveguide. Equation (1) shows that FSR $\Delta\nu_i$ is inversly propotional to the loop length Λ_i. According to the vernier principle, the FSR of MPRR $\Delta\nu$ can be represented as

$$\Delta\nu = N\Delta\nu_1 = M\Delta\nu_2 = L\Delta\nu_3 \tag{2}$$

where L, M and N must be relatively prime numbers. The graphical explanation of eq.(2) is illustrated in Fig.2. Figure 2(a) shows a series of L, M and N which satisfy vernier condition.

Figure 2(b) shows a case when a series of L, M and N has the common factor of 2. This implies that FSR of the MPRR is not $N\Delta\nu_1$ but $(N/2)\Delta\nu_1$.

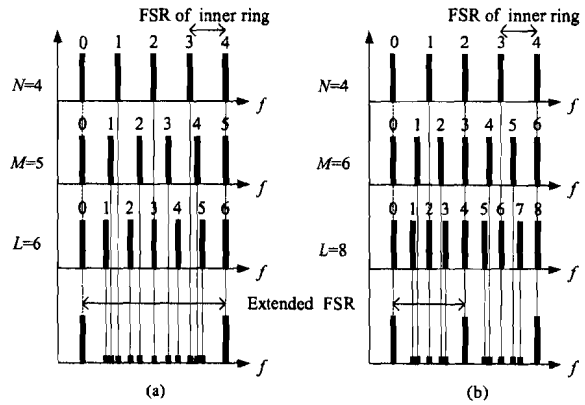

Figure 2: Schematic explanation of vernier principle in the MPRR for two examples (a) $L = 6, M = 5$ and $N = 4$ (the case of relatively prime numbers) and (b) $L = 8, M = 6$ and $N = 4$ (the case of common factor 2).

3 DERIVATION OF TRANSFER FUNCTION

3.1 TRANSFER MATRIX OF CASCADED BLOCKS

In order to derive the transfer function of the MPRR we devide the MPRR into several sections as shown in Fig.3(a), where four-port networks are formed by two sections. There are two four-port network components formed the MPRR, i.e. directional coupler component and double delay-line component (Fig.3(b)). Subscripts u, v and w show the waveguide label. The label u is for straight input-output waveguide, and the labels v and w are for outer and inner ring, respectively. The section number from (1) to (12) denote the reference planes at input and output of four-port network.

According to the notations in Fig.3(b), we can write the transfer matrix expression of each four-port network in terms of complex amplitude of input pairs at p-th section and complex amplitude

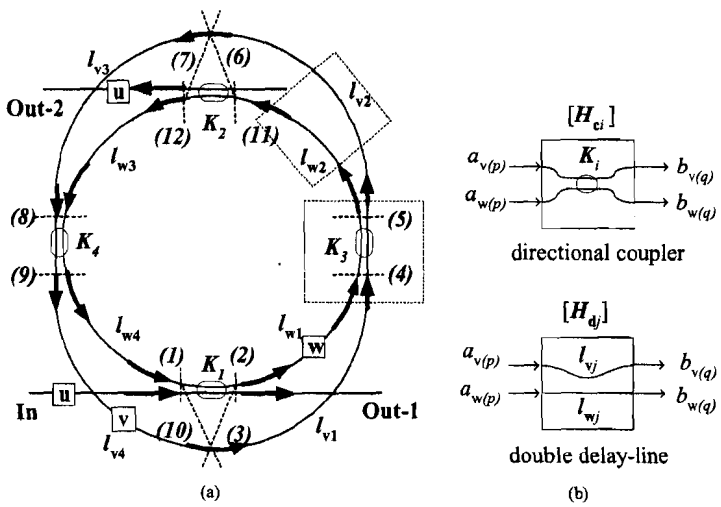

Figure 3: (a) Schematic diagram of MPRR for analysis by means of transfer matrix formulation and (b) Schematic diagram of directional coupler and double delay-line.

of output pairs at q-th section:

(i). Matrix notation for directional couplers with power coupling ratios K_1 and K_2:

$$\begin{bmatrix} b_{u(q)} \\ b_{w(q)} \end{bmatrix} = [H_{ci}] \begin{bmatrix} a_{u(p)} \\ a_{w(p)} \end{bmatrix} \qquad i = 1, 2. \tag{3}$$

(ii). Matrix notation for directional couplers with power coupling ratios K_3 and K_4:

$$\begin{bmatrix} b_{v(q)} \\ b_{w(q)} \end{bmatrix} = [H_{ci}] \begin{bmatrix} a_{v(p)} \\ a_{w(p)} \end{bmatrix} \qquad i = 3, 4. \tag{4}$$

(iii). Matrix notation for double delay-line:

$$\begin{bmatrix} b_{v(q)} \\ b_{w(q)} \end{bmatrix} = [H_{dj}] \begin{bmatrix} a_{v(p)} \\ a_{w(p)} \end{bmatrix} \qquad j = 1, 2, 3, 4. \tag{5}$$

In eqs.(3)-(5), $[H_{ci}]$ is transfer matrix of i-th directional coupler with power coupling ratio K_i ($i = 1, 2, 3, 4$) and $[H_{dj}]$ is transfer matrix of j-th double delay-line ($j = 1, 2, 3, 4$). The transfer matrices of directional couplers and double delay-lines are defined as

$$\begin{cases} [H_{ci}] = \sqrt{1-\gamma} \begin{bmatrix} \sqrt{1-K_i} & -\mathrm{j}\sqrt{K_i} \\ -\mathrm{j}\sqrt{K_i} & \sqrt{1-K_i} \end{bmatrix} \equiv \begin{bmatrix} A_{Ki} & B_{Ki} \\ C_{Ki} & D_{Ki} \end{bmatrix} & i = 1, 2, 3, 4 \\ [H_{dj}] = \begin{bmatrix} \mathrm{e}^{-\mathrm{j}(\beta+\mathrm{j}\alpha)l_{vj}} & 0 \\ 0 & \mathrm{e}^{-\mathrm{j}(\beta+\mathrm{j}\alpha)l_{wj}} \end{bmatrix} & j = 1, 2, 3, 4 \end{cases} \tag{6}$$

where $\mathrm{j}=\sqrt{-1}$. Equation (6) is formulated under a hypothesis that directional couplers have unidirectional power flow and that they have no backward reflection. We assume that directional couplers have same fractional power loss γ and that both rings have same propagation constant β. To facilitate the derivation, we suppose that the inner ring and the outer ring have same attenuation coefficient α. Using blocks represented in Fig.3(b), we can rewrite the MPRR as shown in Fig.4. Since input port (In) of the MPRR corresponds to $a_{u(1)}$, and output ports of Out-1 and Out-2 correspond to $b_{u(2)}$ and $b_{u(12)}$, respectively, we can express the MPRR in four-port network notation as follows:

$$\begin{bmatrix} b_{u(2)} \\ b_{u(12)} \end{bmatrix} = \begin{bmatrix} H_{11} & H_{12} \\ H_{21} & H_{22} \end{bmatrix} \begin{bmatrix} a_{u(1)} \\ 0 \end{bmatrix} . \tag{7}$$

Our aim is to obtain above transfer matrix components H_{11}, H_{12}, H_{21} and H_{22} in terms of the parameters of power coupling ratios and waveguide lengths.

The first step, we will derive equivalent transfer matrix for the cascade of three blocks from section (3) to (6). It is clear that equivalent transfer matrix between section (3) and (6) can be obtained only by multiplying in reverse order the transfer matrices of each component block [8]. Therefore, we can write

$$\begin{bmatrix} b_{v(6)} \\ b_{w(6)} \end{bmatrix} = [H_{d2}][H_{c3}][H_{d1}] \begin{bmatrix} a_{v(3)} \\ a_{w(3)} \end{bmatrix} . \tag{8}$$

We can apply the same procedure to derive equivalent transfer matrix between section (7) and (10). As a result, these equivalent matrices are as follows:

$$\begin{cases} [H_1] \equiv [H_{d2}][H_{c3}][H_{d1}] = \begin{bmatrix} A_1 & B_1 \\ C_1 & D_1 \end{bmatrix} \\ [H_2] \equiv [H_{d4}][H_{c4}][H_{d3}] = \begin{bmatrix} A_2 & B_2 \\ C_2 & D_2 \end{bmatrix} \end{cases} \tag{9}$$

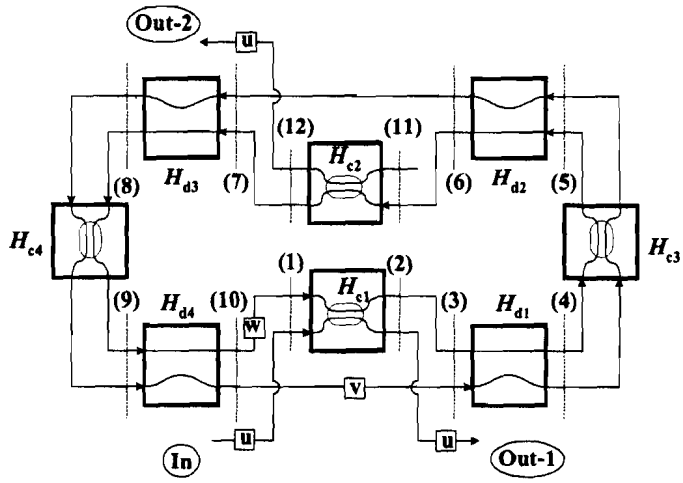

Figure 4: Block diagram of the MPRR which consists of the cascades of directional couplers and double delay-lines.

where $[H_1]$ and $[H_2]$ are equivalent transfer matrices of cascade block between section (3) and (6) and between section (7) and (10), respectively. Restructuring signal block with signal flow-chart method will be described at the following section.

3.2 SIGNAL FLOW-CHART METHOD

Let us see Fig.4 again. Section (3) and section (10) have a common input-output port. The same case is also founded in section (6) and section (7). Therefore, matrix components of $[H_1]$ and $[H_2]$ can be connected as shown in Fig.5. This connection will produce a new equivalent transfer matrix $[H_3]$ again. In order to derive $[H_3]$, using signal flow-chart method is simpler compared with chain matrix operation reported in [6]. Figure 6 illustrates signal flow connections between $[H_1]$ and $[H_2]$.

Based on the Fig.6(b), we can derive ABCD matrix $[H_3]$ using simultaneous equations as follows:

(i). Formulate equation for $b_{w(6)}$ in terms of $a_{w(3)}$ and $a_{v(3)}$:

$$b_{w(6)} = D_1 a_{w(3)} + C_1 a_{v(3)} \ . \tag{10}$$

(ii). Formulate equation for $a_{v(3)}$ in terms of $a_{v(7)}$ and $a_{w(7)}$:

$$a_{v(3)} = B_2 a_{w(7)} + A_2 a_{v(7)} \ . \tag{11}$$

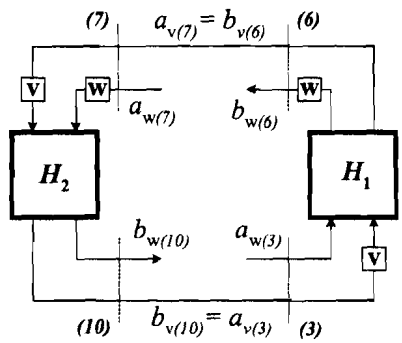

Figure 5: Block diagram of the MPRR rewritten using $[H_1]$ and $[H_2]$.

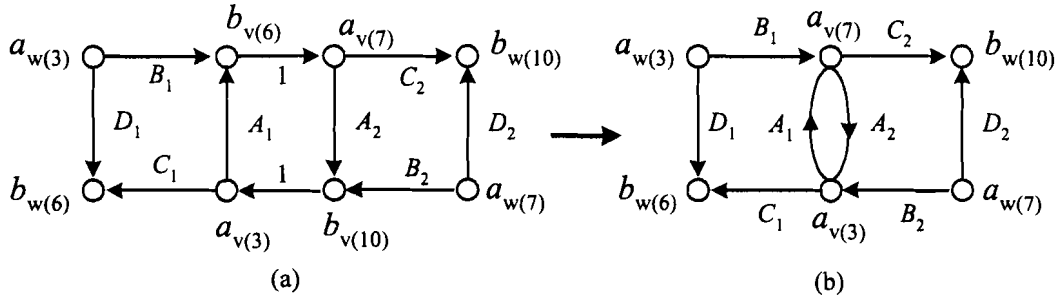

Figure 6: Signal flow-chart of connection between $[H_1]$ and $[H_2]$.

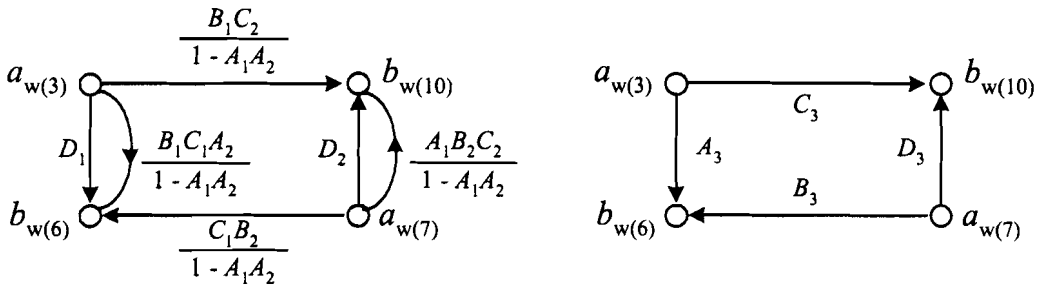

Figure 7: (a) Representation of eqs.(14) and (17), (b) Final signal flow-chart of $[H_3]$.

(iii). Formulate equation for $a_{v(7)}$ in terms of $a_{w(3)}$ and $a_{v(3)}$:

$$a_{v(7)} = B_1 a_{w(3)} + A_1 a_{v(3)} \ . \tag{12}$$

(iv). Substitute eq.(12) into eq.(11), then rewrite $a_{v(3)}$ in terms of $a_{w(3)}$ and $a_{w(7)}$:

$$a_{v(3)} = \frac{B_1 A_2}{1 - A_1 A_2} a_{w(3)} + \frac{B_2}{1 - A_1 A_2} a_{w(7)} \ . \tag{13}$$

(v). Substitute eq.(13) into eq.(10), then rewrite $b_{w(6)}$ in terms of $a_{w(3)}$ and $a_{w(7)}$:

$$b_{w(6)} = \left\{ D_1 + \frac{B_1 C_1 A_2}{1 - A_1 A_2} \right\} a_{w(3)} + \frac{C_1 B_2}{1 - A_1 A_2} a_{w(7)} \ . \tag{14}$$

(vi). Formulate equation for $b_{w(10)}$ in terms of $a_{w(7)}$ and $a_{v(7)}$:

$$b_{w(10)} = D_2 a_{w(7)} + C_2 a_{v(7)} \ . \tag{15}$$

(vii). Substitute eq.(11) into eq.(12) :

$$a_{v(7)} = \frac{B_1}{1 - A_1 A_2} a_{w(3)} + \frac{A_1 B_2}{1 - A_1 A_2} a_{w(7)} \ . \tag{16}$$

(viii). Substitute eq.(16) into eq.(15), then rewrite $b_{w(10)}$ in terms of $a_{w(3)}$ and $a_{w(7)}$:

$$b_{w(10)} = \frac{B_1 C_2}{1 - A_1 A_2} a_{w(3)} + \left\{ D_2 + \frac{A_1 B_2 C_2}{1 - A_1 A_2} \right\} a_{w(7)} \ . \tag{17}$$

Equations (14) and (17) can be represented in signal flow-chart notation as shown in Fig.7(a). Finally, the cascade between $[H_1]$ and $[H_2]$ can be represented as shown in Fig.7(b). Therefore, the equivalent transfer matrix of Fig.7(b) can be written as follows:

$$\begin{bmatrix} b_{w(6)} \\ b_{w(10)} \end{bmatrix} = [H_3] \begin{bmatrix} a_{w(3)} \\ a_{w(7)} \end{bmatrix} = \begin{bmatrix} A_3 & B_3 \\ C_3 & D_3 \end{bmatrix} \begin{bmatrix} a_{w(3)} \\ a_{w(7)} \end{bmatrix}, \tag{18}$$

where

$$\begin{cases} A_3 = D_1 + \dfrac{B_1 C_1 A_2}{1 - A_1 A_2} \\ B_3 = \dfrac{C_1 B_2}{1 - A_1 A_2} \\ C_3 = \dfrac{B_1 C_2}{1 - A_1 A_2} \\ D_3 = D_2 + \dfrac{A_1 B_2 C_2}{1 - A_1 A_2} \end{cases}. \tag{19}$$

The second step is derivation of equivalent transfer matrix as a result of connection between $[H_3]$ and input directional-coupler with power coupling ratio K_1. This derivation is also solved by signal flow-chart method as shown in Fig.8. The ABCD component of Fig.8 can be formulated by using similar procedure described above:

$$\begin{cases} A_4 = A_{K1} + \dfrac{B_{K1} C_{K1} C_3}{1 - D_{K1} C_3} \\ B_4 = \dfrac{B_{K1} D_3}{1 - D_{K1} C_3} \\ C_4 = \dfrac{C_{K1} A_3}{1 - D_{K1} C_3} \\ D_4 = B_3 + \dfrac{D_{K1} A_3 D_3}{1 - D_{K1} C_3} \end{cases}. \tag{20}$$

The last step, the equivalent transfer matrix of the MPRR can be derived as a result of cascade of output directional-coupler with power coupling ratio K_2 and ABCD matrix in eq.(20). The signal flow-chart of this cascade is shown in Fig.9. Finally, the transfer matrix of the MPRR can be written as follows:

$$\begin{bmatrix} b_{u(2)} \\ b_{u(12)} \end{bmatrix} = \begin{bmatrix} H_{11} & H_{12} \\ H_{21} & H_{22} \end{bmatrix} \begin{bmatrix} a_{u(1)} \\ a_{u(11)} \end{bmatrix} \tag{21}$$

where

$$\begin{cases} H_{11} = A_4 + \dfrac{B_4 C_4 D_{K2}}{1 - D_4 D_{K2}} \\ H_{12} = \dfrac{B_4 C_{K2}}{1 - D_4 D_{K2}} \\ H_{21} = \dfrac{C_4 B_{K2}}{1 - D_4 D_{K2}} \\ H_{22} = B_{K2} + \dfrac{D_4 B_{K2} C_{K2}}{1 - D_4 D_{K2}} \end{cases}. \tag{22}$$

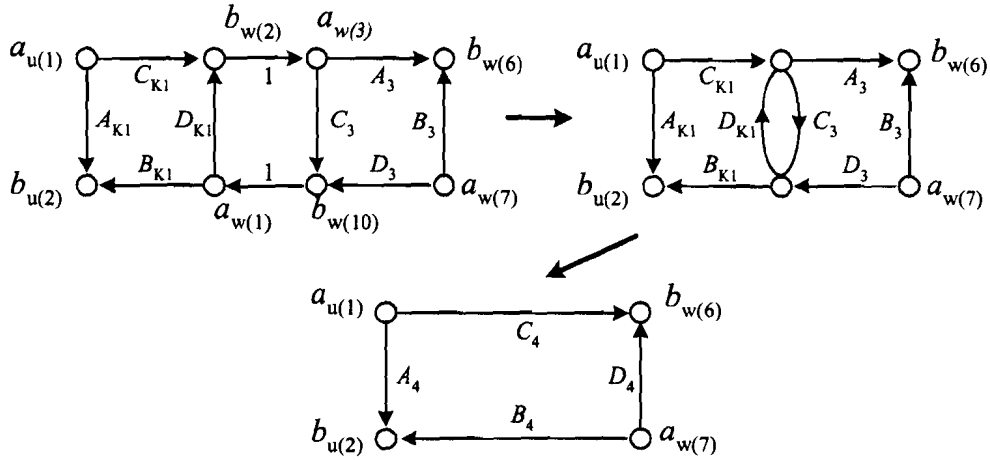

Figure 8: Derivation of $[H_4]$ based on signal flow-chart.

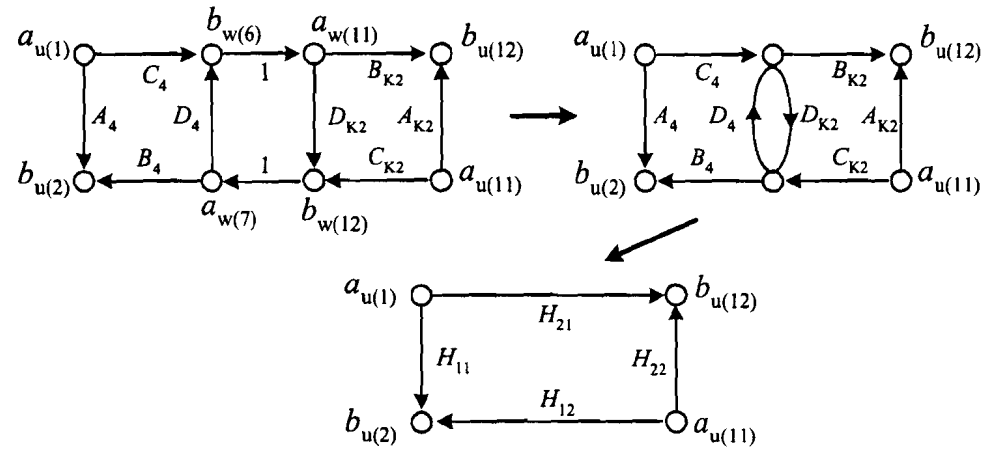

Figure 9: Derivation of H_{11}, H_{12}, H_{21} and H_{22} based on signal flow-chart.

The power transmittance equations of anti-resonance output T_1 and resonance output T_2 (they correspond to Out-1 and Out-2 in Fig.1, respectively) can be obtained by substituting $a_{u(11)}$=0 into eq.(21):

$$T_1 = \left|\frac{b_{u(2)}}{a_{u(1)}}\right|^2 = |H_{11}|^2 \tag{23}$$

$$T_2 = \left|\frac{b_{u(12)}}{a_{u(1)}}\right|^2 = |H_{21}|^2 \tag{24}$$

4 CALCULATION EXAMPLES

4.1 CALCULATION TIME

Previously, we have analyzed single ring-resonator using scattering matrix. By using 550MHz CPU (K6-2) with 192MB memory, we tested to compare calculation time between scattering matrix method and transfer matrix with signal flow-chart method. In the scattering matrix method,

calculation time depends on the value of power coupling ratio, but not for transfer matrix with signal flow-chart method. The comparing result shows that scattering matrix method needs calculation time 3 seconds and 23 seconds for power coupling ratios $K_1 = K_2 = 0.01$ and $K_1 = K_2 = 0.001$, respectively. However, transfer matrix with signal flow-chart method needs only 1 second for both values of power coupling ratio. This calculation time is time to produce 5000 points.

4.2 TRANSMITTANCE CHARACTERISTICS OF THE MPRR

In this section, we show a brief analysis example of the MPRR. Firstly, in order to obtain transmittance characteristics of the MPRR, we need to find resonance condition of the MPRR. We set lengths $l_{w1} = l_{w2} = l_{w3} = l_{w4} \equiv l_{in} = \pi r/2$, and $l_{v1} = l_{v2} = l_{v3} = l_{v4} \equiv l_{out}$. By taking K_3 as a reference, the length of the closed loops denoted by Λ_1, Λ_2 and Λ_3 can be written as the following equations:

$$\begin{cases} \Lambda_1 = 4l_{in} \\ \Lambda_2 = 2l_{in} + 2l_{out} \\ \Lambda_3 = 4l_{out} \end{cases} \tag{25}$$

Therefore, resonance behaviour will occur if phase delays of each closed loop satisfy the following equations:

$$\begin{cases} \beta(4l_{in}) = 2\pi N \cdot N_c \\ \beta(2l_{in} + 2l_{out}) = 2\pi M \cdot N_c \\ \beta(4l_{out}) = 2\pi L \cdot N_c \end{cases} \tag{26}$$

where N_c is the greatest common divisor of resonant number at each loop. According to the vernier principle described in Fig.2 and eq.(2), the FSR of MPRR can be extended if L, M and N are relatively prime numbers.

According to eq.(2), N, M and L also show multiplying numbers of FSR at each closed loop. Since N corresponds to FSR multiplying in the inner ring, we can say N as extension factor of FSR in the MPRR. Equation (26) will results

$$\begin{cases} L + N = 2M \\ l_{out} = \dfrac{L}{N} l_{in} \end{cases} \tag{27}$$

Figure 10 shows a sample output from Out-2 (T_2) for extension factor $N = 10$ (we set $L = 12$ and $M = 14$). Other parameters are $K_1 = K_2 = 10^{-6}, K_3 = K_4 = 10^{-4}$. In this analysis we set $\alpha = 0$, $\gamma = 0$. The FSR of inner ring is 200GHz.

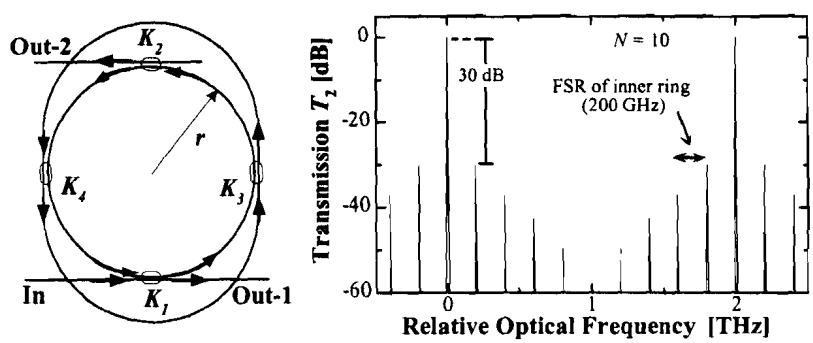

Figure 10: Transmission characteristics of the MPRR at Out-2 port for $N = 10, K_1 = K_2 = 10^{-6}$ and $K_3 = K_4 = 10^{-4}$.

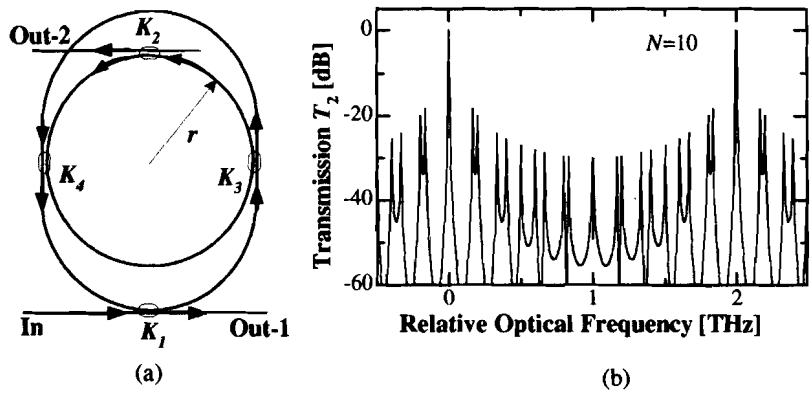

Figure 11: (a) The MPRR structure with directional coupler with power coupling ratio K_1 coupled to outer ring, (b) Power transmittance for (a).

Using signal flow-chart, other structures of the MPRR also can be analyzed simply. Figure.11 shows calculation result for the MPRR structure showed in Fig.11(a). This flexibility is very important to evaluate many types of ring-resonator structure.

5 CONCLUSION

The analysis method for evaluating chacateristics of the MPRR by means of transfer matrix method with signal flow-chart was described. Using this method, even though the structure of the MPRR has various light-paths, matrix components of transfer function can be formulated clearly. As a result, evaluation of the MPRR was performed simply and took a short time compared with scattering matrix method. It is expected that other types of the MPRR can also be analyzed simply.

REFERENCES

[1] D. Rafizadeh, *et al.*, *Opt. Lett.*, **22**, pp.1244-1246, 1997.

[2] Sai T. Chu, *et al.*, *IEEE Photon. Technol. Lett.*, **11**, pp.691-693, 1999.

[3] I.S. Hidayat, *et al.*, *The Extend. Abs. (The 62nd Autumn Meet.) of JSAP*, p.897, 2001.

[4] I.S. Hidayat, *et al.*, *Optics Japan 2001.*, pp.243-244, 2001.

[5] K. Oda, *et al.*, *J. Lightwave Technol.*, **9**, pp.728-736, 1991.

[6] G. Barbarossa, *et al.*, *J. Lightwave Technol.*, **13**, pp.148-157, 1995.

[7] S.C. Hagness, *et al.*, *J. Lightwave Technol.*, **15**, pp.2154-2165, 1997.

[8] B. Moslehi, *et al.*, *Proc. IEEE*, **72**, pp.909-930, 1984.